ISSN 0735-2727, Radioelectronics and Communications Systems, 2021, Vol. 64, No. 1, pp. 45–52. © Allerton Press, Inc., 2021.
Russian Text © The Author(s), 2021, published in Izvestiya Vysshikh Uchebnykh Zavedenii, Radioelektronika, 2021, Vol. 64, No. 1, pp. 51–60.

# Prediction of Rain Attenuation Trend due to Climate Change in Some Locations of Southwestern Nigeria

**Folasade Abiola Semire[1*], Adeyanju Joshua Adekunle[1**], Robert Oluwayimika Abolade[1***], and Oluwole Abiodun Adegbola[1****]**

[1]*Ladoke Akintola University of Technology, Ogbomoso, Nigeria*
**ORCID 0000-0003-0679-7746, e-mail: fasemire@lautech.edu.ng*
***e-mail: adekunleadeyanju153@gmail.com*
****e-mail: roabolade@lautech.edu.ng*
*****e-mail: oaadegbola@lautech.edu.ng*

Received May 6, 2019
Revised October 6, 2020
Accepted November 6, 2020

**Abstract**—Climate change has become a phenomenon of global concern and it has resultant effect on the variability of radio propagation. In recent times, the issue of climate change has been a global phenomenon having its resultant effect on the variability of radio propagation. High-capacity radio signal fades due to absorption by atmospheric gases and scattering by hydrometeors which limits the link availability. This study is aimed at investigating the effects of climate change trend via rain attenuation along the satellite-earth path over Nigeria's climate. Rain rates computed by using the compensated function on Semire and Rosmiwati model were utilized to estimate rain attenuations and effective path lengths using ITU-R P.618-13 model on NIGCOMSAT-1R satellite at 0.01% exceedance for selected frequencies within Ku- and K-bands. Linear trend models for annual rain attenuation were also developed. At 0.01% time unavailability, the prediction of rain attenuation on NIGCOMSAT-1R link using ITU-R P.618-13 model ranged from 14 to 28 dB at Ku-band, and rose beyond 40 dB at K-band. This study inferred that trends of rain rate distributions corresponded to the trends in attenuation due to rain and then concluded that the rising trends of yearly signal outage along earth-space path as a result of increasing rainfall intensity was due to climate change in the study area. This outcome can be explored for better communication planning and design in order to provide reliable links in order to satisfy customers' demand for high quality radio communication.

**DOI:** 10.3103/S0735272721010052

## 1. INTRODUCTION

Wireless communication is essential in global technological systems and climate change is a key factor most likely to be considered during the radio and telecommunications planning. Communication systems operating at frequencies of microwave and millimeter bands may experience a link failure at certain times due to the rain attenuation, which temporarily makes the link unavailable for use [1].

As the climate varied over the years with significant changes, radio and telecommunications systems have become more sensitive to climatic parameters, especially rain. The global climate has been indisputably changing over the last few decades, and it will most likely continue changing in coming decades, with direct effect on precipitation, which in turn brings about a significant impact on radio propagation [2].

Although regional effects of climate change vary depending on the location of regions, there is no doubt that precipitations are on the rise [3]. Therefore, radio and telecommunications planning has necessitated a thorough study in electromagnetic wave propagation.

Taken together, the cloud and precipitation particles are identified as hydrometeors which affect radio systems operating at frequencies 10 GHz and above [4]. Rain occurrence constitutes a major impairment factor due to absorption and scattering of radio waves; resulting in signal attenuation and the overall system availability reduction, and the degradation of system performance.

Hydrometeors in the form of rainfall dominate the influence of the atmosphere on the satellite transmission [5]. This disruption comes in form of attenuation. The attenuation of signals at the atmospheric

**Table 1.** Geographical parameters of locations of study

| Location | Longitude, deg | Latitude, deg | Height above sea level, m | Mean annual accumulated rainfall, mm | Observation period, years |
|---|---|---|---|---|---|
| Abeokuta | 3.35 | 7.16 | 66 | 1299.81 | 33 |
| Ibadan | 3.91 | 7.39 | 230 | 1380.27 | 28 |
| Itoikin | 3.79 | 6.65 | 43 | 1245.69 | 27 |
| Sepeteri | 3.65 | 8.63 | 348 | 1257.95 | 21 |
| Iseyin | 3.60 | 7.37 | 308.22 | 1193.78 | 21 |
| Saki | 3.38 | 8.67 | 457 | 1165.99 | 21 |

layer is predominant and it could be predicted by the use of complex permittivity from the field theory and employed in the design of communication link system.

The excess attenuation due to rainfall becomes one of the most important limits of Line of Sight (LOS) microwave links performance above a certain threshold of frequency [6]. Therefore, the more intense is the rainfall, the deeper the attenuation becomes, thereby making it a dominant factor of consideration in radio propagation in which rainfall rate depends on the liquid water content and the velocity of the falling drops [7].

## 2. BACKGROUND OF STUDY AREA AND DATA COLLECTION

Nigeria, which lies between longitude 2°E and 15°E and latitude 4°N and 14°N has about 910.77 km$^2$ of its total area covered by land mass. The Nigerian climate is dominated by the influence of the Tropical Maritime air mass and the Tropical Continental air mass.

According to the CHIRPS rainfall dataset [8], May–October rainfall ranges widely across the country with total rainfall being the highest in the south where more than 1,400 mm are received; the central part of Nigeria receives 800–1,200 mm while the Northern areas receive less than 800 mm, with some northeastern areas bordering Niger and Chad receiving less than 400 mm. They added [8] that the total rainfall has increased by more than 50 mm across most part of the country since the 1980s, and the total May–October rainfall has increased by more than 30% while this figure for localized areas of the west has increased by 10–15%.

The locations of study fall within three states of the Southwest region of Nigeria which are Abeokuta (Ogun State), Itoikin (Lagos State), and Ibadan, Iseyin, Saki, and Sepeteri (Oyo State). This region lies within the rain forest climatic zone and has rugged topography with annual mean temperature during the day varying while rainfall falls within 928 mm and 3240 mm per year, the relative humidity ranging between 65 and 75%.

Basically, this region has two seasons, which are dry season (mostly from November to February) and wet season (within the rest of the calendar year). Rainfall at the locations of study is usually observed during the wet season with short interruption usually experienced in August, but heavy rain is usually resuming in September [9], [10], hence providing for the tropical rainfall pattern with seasonal distribution.

Rainfall data for the period from 21 to 33 years was obtained from Weather Stations as provided by the Nigerian Meteorological Agency (NIMET), the Federal Government Agency in charge of Weather parameters and atmospheric conditions in Nigeria, and also from the Ogun-Osun River Basin Development Authority (OORBDA). The obtained data are based on monthly integration time, which according to [11] may be adequate for providing enough information for rainfall estimation for the purpose of attenuation prediction along terrestrial or satellite communications link. The locations and their geographical parameters are presented in Table 1.

## 3. METHODOLOGY

Leveraging on the rain rate model of Semire and Rosmiwati [12], which was generated from rainfall data of Ogbomoso, the rain rates at one minute integration time for values 1, 0.1, 0.01, 0.001% of time exceedances have been utilized to generate cumulative distributions functions (CDFs) for the rain rate of the locations in question using the curve-fitting tool of MATLAB 2013a [13].

A correction factor (CF) of model having the form:

$$\mathrm{CF} = a\exp(bp) + \frac{c}{p^{d}}\exp(ep),$$

was introduced into the rain rate CDFs with the coefficients of the six locations being averaged as follows [13]:

$$a = 0.612283,\ b = 1.248733,\ c = 0.074348,$$

$$d = 0.3546,\ e = 2.359.$$

Rain attenuation exceeded at 0.01% of the time of year was estimated from the average one-minute rain intensity using ITU-R Rec. P.618-13 [14], [15], with its adjustment factor, which has wide international acceptability. This model was used as a benchmark for estimating the induced attenuation. It utilizes the site parameters, namely: latitude, longitude, altitude of the station, frequency, the percentage exceedance and the one-minute-integration-time rainfall rate. The rain attenuation for NIGCOMSAT-1R (Longitude 42.5°E) was estimated by first computing the specific attenuation along the earth-space path.

Due to the proportionality of rain rate to attenuation, the trend function can forecast the possible yearly attenuation. Basically, these might be indicating increased attenuation as a result of the rising rainfall, owing to the global climate change. The outage patterns based on the attenuation prediction might probably follow the identified trends. For the application of trend and variability to the dimensioning of radio links, it is reasonably feasible that the trend can account for the outcome of long-term duration of yearly rainfall events so as to examine local changes, then identify and analyze the trends in rain attenuation at 0.01% exceedance.

Annual rain attenuation, corresponding to the statistics of one-minute integration time rain rate at 0.01% exceedance, was plotted against year for the locations in question to compare and evaluate possible trends due to the rainfall intensity for the entire period of years under consideration. This is in order indicate the uniformity or variability in distribution.

### *3.1. Trend of Outage due to Yearly Rainfall Variability*

This evaluation was done by using the coefficient of variation (CV) and correlation coefficient ($r$). CV is given as:

$$\mathrm{CV} = \frac{\sigma}{\overline{A}} \times 100\%,$$

where $\overline{A}$ is the mean value of each attenuation distribution, $\sigma$ is the standard deviation from the mean of the distribution.

Also, the correlation coefficient $r$ is defined as follows:

$$r = \frac{\frac{1}{N}\sum (Y \times A) - (\overline{Y} \times \overline{A})}{\sigma_Y \sigma_A},$$

where $N$ is total number of observations in the distribution series, $A$ is the individual annual attenuation in the distribution series, $Y$ is the year, $\sigma_Y$ is the standard deviation of $Y$, $\sigma_A$ is the standard deviation of $A$.

**Table 2.** Geo-characteristic parameters for locations using Nigcomsat-1R satellite

| Location | Mean rain rate at 0.01%, mm/h | Isotherm height, km | Rain height, km | Elevation angle, deg | Tilt angle, deg | Polarization angle, deg | Specific attenuation, dB/km |
|---|---|---|---|---|---|---|---|
| Abeokuta | 105.40 | 4.52 | 4.88 | 26.70 | 78.75 | 45.26 | 3.30 |
| Ibadan | 109.32 | 4.52 | 4.88 | 27.48 | 78.27 | 46.07 | 3.49 |
| Itoikin | 103.69 | 4.51 | 4.87 | 27.34 | 79.44 | 46.71 | 3.97 |
| Sepeteri | 102.79 | 4.52 | 4.88 | 26.86 | 76.40 | 44.77 | 3.30 |
| Iseyin | 102.70 | 4.52 | 4.88 | 26.99 | 78.37 | 44.91 | 3.27 |
| Saki | 101.87 | 4.52 | 4.88 | 26.48 | 76.42 | 46.46 | 4.95 |

**Table 3.** Attenuation estimation at 0.01% exceedance using ITU-R P.618-13 model at varied frequencies

| Frequency, GHz | Rain attenuation, dB | | | | | |
|---|---|---|---|---|---|---|
| | Abeokuta | Ibadan | Itoikin | Sepeteri | Iseyin | Saki |
| 10.00 | 14.51 | 14.31 | 14.42 | 13.84 | 13.94 | 14.34 |
| 11.00 | 17.65 | 17.40 | 17.54 | 16.84 | 16.95 | 17.42 |
| 12.00 | 21.03 | 20.74 | 20.91 | 20.08 | 20.21 | 20.74 |
| 12.52 | 22.83 | 22.52 | 22.71 | 21.81 | 21.94 | 22.51 |
| 12.63 | 23.20 | 22.89 | 23.08 | 22.16 | 22.30 | 22.87 |
| 12.68 | 23.38 | 23.06 | 23.25 | 22.33 | 22.47 | 23.05 |
| 14.00 | 28.01 | 27.64 | 27.87 | 26.77 | 26.93 | 27.60 |
| 18.80 | 45.14 | 44.62 | 44.97 | 43.23 | 43.41 | 44.45 |
| 19.45 | 47.57 | 47.03 | 47.40 | 45.57 | 45.75 | 46.84 |
| 20.00 | 49.65 | 49.09 | 49.48 | 47.58 | 47.75 | 48.89 |
| 20.20 | 50.42 | 49.85 | 50.24 | 48.31 | 48.49 | 49.64 |
| 25.00 | 69.38 | 68.66 | 69.19 | 66.54 | 66.74 | 68.28 |
| 30.00 | 89.34 | 88.42 | 89.13 | 85.72 | 85.95 | 87.83 |

From the evaluation of the yearly distribution, insight into how the climate has been changing can be deduced and trends of attenuation evolution due to the change in climate can be inferred. Thus, a possible outage pattern for the coming years can be predicted via expected fade margins towards the future.

## 4. RESULTS

In order to determine the attenuation on this NIGCOMSAT-1R satellite, the specific attenuation and the path length through the troposphere were calculated for the six locations. The geo-characteristic parameters of Nigcomsat-1R satellite for each location are shown in Table 2.

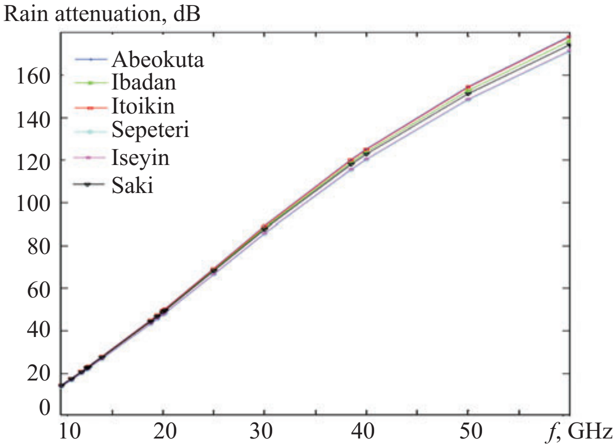


**Fig. 1.** Rain attenuation for locations at 0.01% exceedance using ITU-R P.618-13 model.

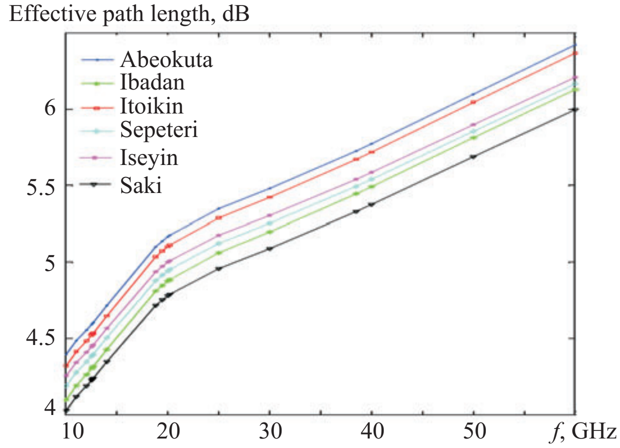


**Fig. 2.** Effective path length for locations at 0.01% exceedance using ITU-R P.618-13 model.

**Table 4.** Effective path length estimation at 0.01% exceedance using ITU-R P.618-13 model at varied frequencies

| Frequency, GHz | Effective path length, km | | | | | |
|---|---|---|---|---|---|---|
| | Abeokuta | Ibadan | Itoikin | Sepeteri | Iseyin | Saki |
| 10.00 | 4.40 | 4.10 | 4.32 | 4.19 | 4.26 | 4.03 |
| 11.00 | 4.49 | 4.19 | 4.41 | 4.28 | 4.34 | 4.12 |
| 12.00 | 4.56 | 4.27 | 4.49 | 4.35 | 4.41 | 4.19 |
| 12.52 | 4.59 | 4.30 | 4.52 | 4.39 | 4.45 | 4.23 |
| 12.63 | 4.60 | 4.31 | 4.53 | 4.39 | 4.46 | 4.24 |
| 12.68 | 4.61 | 4.32 | 4.54 | 4.40 | 4.46 | 4.24 |
| 14.00 | 4.72 | 4.43 | 4.65 | 4.51 | 4.57 | 4.35 |
| 18.80 | 5.10 | 4.81 | 5.04 | 4.88 | 4.94 | 4.72 |
| 19.45 | 5.14 | 4.85 | 5.08 | 4.92 | 4.97 | 4.75 |
| 20.00 | 5.17 | 4.88 | 5.10 | 4.94 | 5.00 | 4.78 |
| 20.20 | 5.18 | 4.89 | 5.11 | 4.95 | 5.01 | 4.79 |
| 25.00 | 5.35 | 5.06 | 5.29 | 5.12 | 5.18 | 4.96 |
| 30.00 | 5.48 | 5.20 | 5.42 | 5.25 | 5.30 | 5.09 |

### *4.1. Estimation of Rain Attenuation and Effective Path Length at 0.01% Exceedance*

Since the attenuation exceeded at 0.01% of the year is of particular interest for radio dimensioning purposes. The plot of rain attenuation at selected frequencies between 10 and 30 GHz using ITU-R P.618-13 model for the locations is displayed in Fig. 1, while the values of the estimation are shown in Table 3.

The attenuation results reveal that signal degradation due to rain is most severe in Abeokuta, then in Itoikin and followed by Ibadan. This is possibly due to factors such as longitude, latitude, the height above sea level, the elevation angle and the polarization tilt that contributes to signal attenuation.

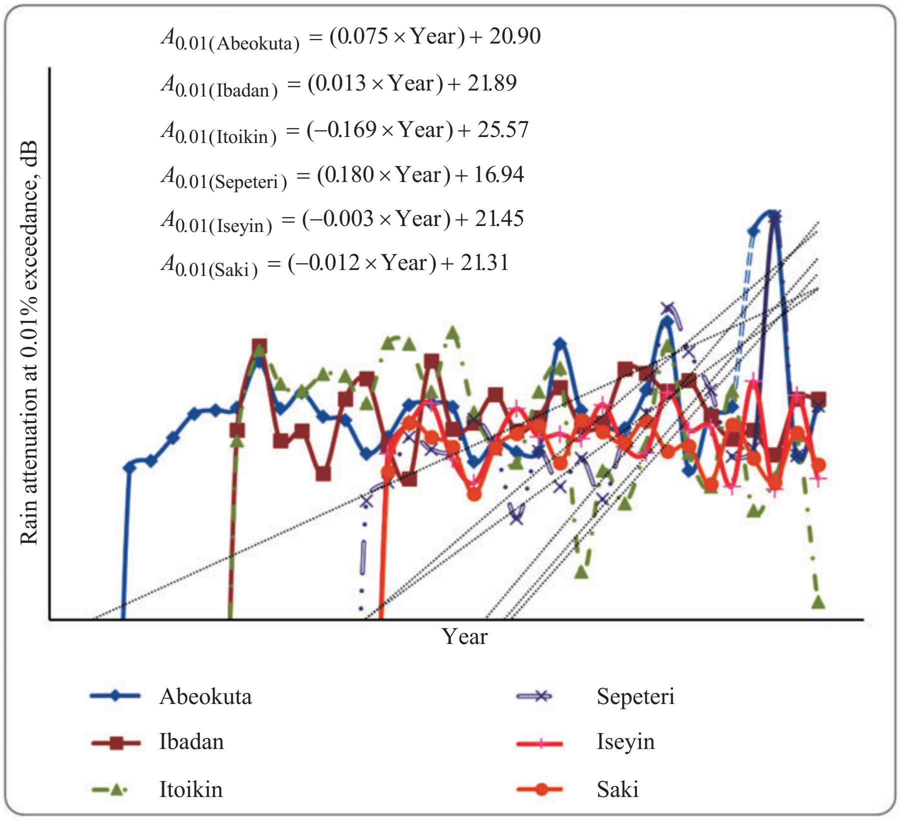


**Fig. 3.** Yearly trend of rain attenuation at 0.01% exceedance for locations.

It was also observed that Iseyin and Sepeteri experienced less rain attenuation because they are relatively farther to the coast. It can also be seen that the higher the frequency, the higher is the signal fade that will be experienced in communication link.

The estimated attenuation at 0.01% unavailability (i.e. about 53 min outage in a year) ranged between 20 and 21 dB at 12 GHz (Ku-band), while it had risen up to 178 dB at 60 GHz (V-band). Therefore, effective mitigation techniques against the rain fade are very important at higher frequencies.

Furthermore, the effective path length for each region was likewise determined and it illustrates the dependency on frequency and elevation angle. This effective length is used due to the fact that the rain density is not uniform as the signal travels through a rainy medium. The plot of the effective path length for the locations at 0.01% unavailability across the frequency bands under consideration is shown in Fig. 2 indicating that the effective path length through rain rises as the frequency increases.

The tabulated results for this effective path length at 0.01% unavailability for the locations are also presented in Table 4. From these results, Abeokuta had the largest length, followed by Itoikin and then Iseyin while Saki had the smallest. The reason for this is due to their height above the mean sea level.

### *4.2. Forecast of Outage Trend for Future Years*

The plot of these trends in which a linear function is employed to illustrate the yearly rain attenuation of the locations over the entire period is shown in Fig. 3. This trend function is of the form:

$$\text{Rain attenuation} = a \times \text{year} + b,$$

where $a$ is the slope of the regression, $b$ is the intercept of the function.

Abeokuta, Ibadan and Sepeteri had positive value of slope which might be suggesting an increasing tendency of yearly rain attenuation, while Itoikin, Iseyin and Saki had a negative slope which is vice versa (i.e. decreasing trend).

**Table 5.** Coefficients of annual rain rate regression trend and variation performance for all locations

| Location | Coefficients of yearly rain rate trend regression | | Variation performance | |
|---|---|---|---|---|
| | *a* | *b* | CV | *r* |
| Abeokuta | 0.075 | 20.90 | 9.03 | 0.89 |
| Ibadan | 0.013 | 21.89 | 5.18 | 0.12 |
| Itoikin | –0.169 | 25.57 | 9.62 | –1.42 |
| Sepeteri | 0.180 | 16.94 | 8.45 | –277.01 |
| Iseyin | –0.003 | 21.45 | 5.21 | –0.02 |
| Saki | –0.012 | 21.31 | 3.69 | –0.09 |

The trend regression coefficients, coefficients of variation (CV) as well as the correlation coefficients obtained are presented in Table 5 for all the locations. Saki had the least CV = 3.69, which implied that its series has minimal deviation from the mean in the distribution and its trend prediction will be the most accurate. The relatively high value of CV for Abeokuta, Itoikin and Sepeteri is largely due to the occasional overshoot off the mean point as a result of extremely high rainfall intensity during certain years within the distribution.

From the correlation coefficient perspective for all locations, Abeokuta gave the best correlation with a value of 0.89 (closest to 1), while that of Sepeteri is the worst with a value of –277.01 largely because some data is not available within the distribution. Also, the negative value of correlation coefficient for Itoikin, Sepeteri, Iseyin, and Saki suggests that the trend of their distributions tends towards the reverse direction of what was indicated by their trend line slopes, thereby implying a rise in attenuation trend as well.

Thus, it can be inferred that the trend of signal degradation, due to the rainfall intensity, is generally on the rise at the locations of study. In the year 2012, the attenuation at 0.01% unavailability for Abeokuta rose to as high as 29 dB. Hence, for a reliable communication link along the satellite (especially NIGCOMSAT-1R), fade margins much higher than the attenuations presented in this work should be designed.

## 5. CONCLUSIONS

Despite the fact that the effective path length agrees with the direct proportionality to the rainfall attenuation, however when considering satellite communication, other dominant factors such as frequency and the local rain rate also contribute to the overall rain attenuation.

Considering the locations of study, the results from this study showed that the general range of attenuation estimation for the zone was between 14 and 28 dB at Ku-band, and rose beyond 40 dB at K-band. Iseyin and Sepeteri experienced less rain attenuation at all frequencies and percentage availabilities, thus they require lower fade margins for satellite link design purposes. Conversely, Abeokuta, Itoikin and Ibadan experienced the most severe signal impairment due to high rainfall intensity, and thereby they require higher fade margins at all frequencies and percentage availabilities.

Also, the rain attenuation increases as frequency rises resulting in an increase of the signal fade depth. However, since there is commensurate proportionality between the rain rate and attenuation, the trends in rain rate distributions translate into trends in signal fade margins due to rain. Therefore, if the fade margin can be increased to exceed the highest rain attenuation estimated, then the links will be outage-free. Hence, there is a need to optimize the available spectrum to obtain satisfactory communication links even with the change in climate.

The outcome of this work can be explored for better communication planning and design in order to provide reliable links to satisfy customers' demand in radio communication such that the service can be made available all-round the year, especially during the rainfalls.

## CONFLICT OF INTEREST

The authors declare that they have no conflict of interest.

## ADDITIONAL INFORMATION

The initial version of this paper in Russian is published in the journal "Izvestiya Vysshikh Uchebnykh Zavedenii. Radioelektronika," ISSN 2307-6011 (Online), ISSN 0021-3470 (Print) on the link http://radio.kpi.ua/article/view/S0021347021010052 with DOI: 10.20535/S0021347021010052.

## REFERENCES

1. S. J. Malinga, "Determination of Millimetric Signal Attenuation due to Rain using Rain Rate and Raindrop Size Distribution Models for Southern Africa" (2014).
2. U. WHO, *Climate Change and Human Health - Risks and Responses* (2003). URL: https://www.who.int/globalchange/publications/cchhsummary/en/.
3. A. Karaburun, A. Demirci, and F. Kora, "Analysis of spatially distributed annual, seasonal and monthly temperatures in Marmara Region from 1975-2006," *Ocean J. Appl. Sci.* **5**, No. 2, 131 (2012).
4. R. K. Crane, *Electromagnetic Wave Propagation through Rain* (John Wiley and Sons,, 1996). URL: https://www.wiley.com/en-ua/Electromagnetic+Wave+Propagation+Through+Rain-p-9780471613763.
5. R. Olsen, D. Rogers, and D. Hodge, "The aR^b relation in the calculation of rain attenuation," *IEEE Trans. Antennas Propag.* **26**, No. 2, 318 (1978). DOI: 10.1109/TAP.1978.1141845.
6. F. Moupfouma, "Improvement of a rain attenuation prediction method for terrestrial microwave links," *IEEE Trans. Antennas Propag.* **32**, No. 12, 1368 (1984). DOI: 10.1109/TAP.1984.1143248.
7. R. L. Freeman, *Radio System Design for Telecommunications*, 2nd ed. (Wiley-Interscience, 1997).
8. J. P. Verdin, "Famine Early Warning System Network (FEWS NET)" (2006). DOI: 10.3133/fs20063022.
9. F. A. Semire and T. I. Raji, "Characteristics of Measured Rainfall Rate at Ogbomoso, Nigeria for Microwave Applications," *J. Telecommun. Inf. Technol.*, No. 2, 85 (2011).
10. T. V. Omotosho and C. O. Oluwafemi, "One-minute rain rate distribution in Nigeria derived from TRMM satellite data," *J. Atmos. Solar-Terrestrial Phys.* **71**, No. 5, 625 (2009). DOI: 10.1016/j.jastp.2009.02.003.
11. G. O. Ajayi, S. Feng, S. M. Radicella, and B. M. Reddy, *Handbook on Radiopropagation Related to Satellite Communications in Tropical and Subtropical Countries* (ICTP, Trieste, Italy, 1996).
12. F. A. Semire and M.-M. Rosmiwati, "Development of rain rate prediction model for Nigeria," *Can. J. Pure Appl. Sci.* **5**, No. 3, 1721 (2011). URL: http://www.cjpas.net/wp-content/uploads/pdfs/5/3/Oct-11_18.pdf.
13. F. Abiola Semire, A. Adekunle, and R. Olayimika Abolade, "A study on rain rate prediction of Southwestern Nigeria," *Phys. Sci. Int. J.*, 1 (2020). DOI: 10.9734/psij/2019/v23i430166.
14. R. ITU-R, "Propagation data and prediction methods required for the design of Earth-space telecommunication systems," in *International Telecommunication Union Radio Communication P.618-13* (Geneva, 2017). URL: https://www.itu.int/dms_pubrec/itu-r/rec/p/R-REC-P.618-13-201712-I!!PDF-E.pdf.
15. F. A. Semire, R. Mohd-Mokhtar, and Z. K. Adeyemo, "Statistical analysis of rain height over Malaysia," *Radioelectron. Commun. Syst.* **59**, No. 9, 423 (2016). DOI: 10.3103/S0735272716090065.